Nigerian Research Journal of Engineering and Environmental Sciences 6(2) 2021 pp. 503-519
p ISSN: 2635-3342; e ISSN: 2635-3350

**Nigerian Research Journal of Engineering and Environmental Sciences**
**Journal homepage: www.rjees.com**

**Original Research Article**

# Preliminary Investigation for Geothermal Energy Resources Applications in Obaretin and Ofumwengbe Communities, Ovia South West, Edo State, Nigeria

***[1]Emeribe, C.N., [1]Aganmwonyi, I., [1]Uwadia, N.O., [1]Igbinomwanhia, D.I. and [1,2]Ogbomida, E.T.**

[1]National Centre for Energy and Environment, Energy Commission of Nigeria, University of Benin, Benin City, Edo State, Nigeria.
[2]Directorate of Research, Innovation and Consultancy, the Copperbelt University, Jambo Drive, Riverside, Kitwe, Zambia.
*emeribe.c@ncee.org.ng

http://doi.org/10.5281/zenodo.5805099

**ARTICLE INFORMATION**

*Article history*:
Received 08 Oct, 2021
Revised 06 Nov, 2021
Accepted 20 Nov, 2021
Available online 30 Dec, 2021

*Keywords*:
EU water scheme
Geothermal energy
Water resources development
Geothermal applications
Small hydropower plant

**ABSTRACT**

*The present study aimed at preliminary investigation of the potentials of developing geothermal energy applications from an existing EU-Niger Delta support borehole project in parts of Ovia-South West Local Government Area, Edo State. Methods adopted were reconnaissance level-survey of existing non-technical infrastructure and field observations. Measured temperature of the boreholes at discharge points were between 47.8 °C and 49.8 °C in Obaretin and Ofumemgbe. Iron (Fe) level exceeded the acceptable limit for drinking with a mean value of 0.3 mg/l, while chromium was slightly higher than permissible limit in Obaretin EU borehole. The elevation at well head at discharge points was 42 m and 40 m in Obaretin and Ofumwengbe respectively. At well outlets elevation were 36 m and 32 m in Obaretin and Ofumwengbe respectively. From pumping test carried out at the borehole locations, the results revealed that Obaretin has an average discharge of 8.9 $m^3$/h (0.00247 $m^3$/s) while the average discharge at Ofumwengbe was estimated to be 8.6 $m^3$/h (0.00234 $m^3$/s). The power potentials of the two locations was estimated to be 116.31 W and 147 W from Obaretin and Ofumwengbe respectively, if hydropower plants are desired in the study area. Based on the temperature of water at discharge point, the study concludes that the hot water from the EU-project is not suitable for electricity generation which requires a temperature of above 200 °C, instead may be harnessed for recreation activities or other direct uses.*



## 1. INTRODUCTION

Nigeria has an abundance of renewable energy sources such as wood, solar, hydropower, and wind (ECN, 2003). In recent years however, while the research and development have intensified towards development of other renewable energy sources (biomass, wind, solar etc) little attention has been given to geothermal

energy resource especially in the developing countries (Oduor, 2010). According to IRENA (2020), geothermal energy is heat derived within the sub-surface of the earth. Depending on its characteristics, geothermal energy can be used for heating and cooling purposes or be harnessed to generate clean electricity. According to DiPippo (1991), geothermal plants are considered as environmentally benign in terms of emissions abatement, water, and land-use as compared with other alternatives such as fossil fuels.

Over the years, due to increasing growing demand for electricity, research and development have intensified in geothermal energy technology especially in the developed countries (Oduor, 2010; EIA, 2021). In 2018, 27 countries, including the United States, generated a total of about 83 billion kWh of electricity from geothermal energy. Indonesia was the second-largest geothermal electricity producer after the United States, at nearly 14 billion kWh of electricity, which was equal to about 5% of Indonesia's total electricity generation (EIA, 2021). By 2019, the total installed capacity for geothermal direct utilization worldwide was 107,727 MWt, being 52.0% increase compared to the 8.7% growing annual compound rate in 2015 (EIA, 2021). According to Lund and Toth, (2020) the recent higher capacity factor and growth rate for annual energy use is due to the increase in geothermal heat pump installations even though they have a low capacity factor of 0.245 worldwide.

In Africa, there are documented progress in geothermal energy development, especially in the eastern part of the continent. The East African nations have successfully harnessed its geothermal capabilities, generating an estimated 630 MW, since 2014 (Dutiro, 2019). Kenya is considered the region's pioneer with an installed capacity of 676MWe (ESI Africa, 2019). Similarly, between 2012 and 2019, Iceland which is a co-financier of the UNEP African Rift Geothermal Development Facility Project, has helped seven countries in East Africa develop their expertise in geothermal energy through the Geothermal Exploration Project (UNEP, 2020). The Infrastructure Consortium for Africa and the United Nations Environment Program has estimated a potential of 20,000 MW of geothermal energy across Eastern Africa, and nations such as Tanzania, Uganda, Rwanda, Djibouti, Eritrea and Comoros have undertaken preliminary exploration for geothermal potential (ESI, Africa, 2020). Ethiopia is currently harnessing its geothermal capacity, and, is aiming to reach 1 GW by 2021. Burundi, Zambia and Uganda are also currently operating small-scale geothermal plants (Dutiro, 2019).

While the development of geothermal energy in African has advanced, most of its applications are for direct uses and heating systems other than for electricity generation. Such applications include hot mineral springs for bathing, cooking, heating, and industrial, green houses planting (e.g flowers, fruits and vegetables), agro-business (fish farms and crop drying) applications etc. In Kenya, for example, the main geothermal uses are: 5.3 MWt and 185 TJ/yr for greenhouses, 0.3 MWt and 9.9 TJ/yr for agricultural drying, 0.2 MWt and 6.5 TJ/yr for fish farming, 8.7 MWt and 275.5 TJ/yr for bathing and swimming, and 4.0 MWt and 125.5 TJ/y, for other uses (laundromat and milk processing), for a total of 18.5 MWt and 602.4 TJ/yr (Omenda *et al.* 2019). In Madagascar, Andrianaivo and Ramasiarinoro, (2015) reported a similar use that is practiced at Ranomafana Namorona Spa near the Ranomafana National Park. Thermal springs in Bezaha Spa and in Betafo Spa are used at the rehabilitation and recreation center. Drinking water out of taps is used for disease prevention. Utilized water for relaxation, sanitary needs and prevention has the highest share in balneology. The total for bathing and swimming is: 2.814 MWt and 75.585 TJ/yr.

In Nigeria, there are sites where the recreational centers were developed on the basis of well- known geothermal springs, and where these springs have direct applications such as the Ikogosi Warm Spring Resort in Ikogosi town, Ekiti State and Wiki Spring Resort in Yankari National Park, Bauchi State (NE Nigeria). The Ikogosi warm spring has a temperature of about 70 $^{o}$C at the source and 37 $^{o}$C after meeting a water stream from another cold spring. There is a swimming pool filled with the water from the spring as well as accommodation facilities for tourist in the resort. The Wikki warm spring has a temperature of 32 $^{o}$C, with a swimming area for the tourists fed by the source in a nearby cave. It is estimated that 0.7 MWt and 14 TJ/yr are the capacity and use of geothermal energy in Nigeria for bathing and swimming (Kwaya and Kurowska, 2020).

In spite of the progress in geothermal energy technology, the utilization of geothermal energy remains relatively low when compared to other non-hydropower renewable energy sources. According to IEA (2013), geothermal energy is projected at about 0.3 percent, with the prospect of growing to 0.5 percent by 2030. Also across the globe, the scale of geothermal power generation is also modest when compared with other renewable energy sources. However, the exploitable geothermal energy potential in some parts of the world is far greater than current utilization, offering scope for significant investment in scale-up (ESMAP, 2012). In South-South Nigeria, there is no documented case of geothermal energy applications. Nevertheless, the recent hot water from EU-Niger Delta Support Programme-Component 3 (Water and Sanitation) in Edo State, presents some evidence of geothermal energy applications, and this justifies the need for the present study.

## 2. MATERIALS AND METHODS

### 2.1. Study Area

The study area is Ovia southwest Local Government Area, which houses the two (2) EU-Niger Delta Support Programme-Component 3 (Water and Sanitation) Projects, one at Obaretin community and the second at Ofunmwegbe community. Obaretin is 40 kilometers from the Ring Road in Benin City. The community extends from Ofunmwegbe along the Benin Lagos express way and shares borders with Iguobanor, Ugbokun, Ofunmwegbe communities. Ovia Southwest lies within the co-ordinate 5.2796903°E 6.5951587°N and 5.4073769°E 6.7347231°N (Figure 1). The elevation ranges between 37 and 66 m above mean sea level with relatively flat and gentle geomorphology. The region consists of surface and ground water resources. The surface water resources include major rivers and streams such as Okada River, Igbogo River, Iguevinyoba river and Siloko river.

Figure 1: Satellite image map of study location

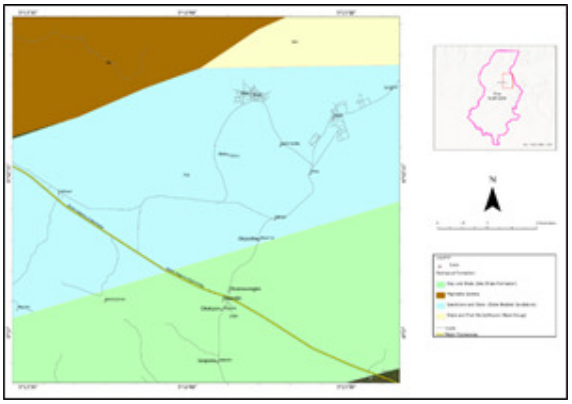

Figure 2: Local geology of the study area (arrowed) (Modified after NGSA)

The geological structure of Edo State composed basically of both crystalline Basement rocks (Precambrian age) occupying the Northern part of the state and sedimentary rocks, spanning from Cretaceous to Recent in age. The sedimentary rock is ubiquitous across the state with major dominance in the south. Figure 2 displays the major local geology or the region. The occurrence of warm ground water resource in this region is of major interest as they occur within very interesting geological settings. The regions consist of clay – shale which is part of the Imo shale outcrop that is an arcuate belt from Western Nigeria to the East. It lies conformably on the Maaestrichtian Abeokuta and Nsukka Formation (Emofurieta *et al.,* 1994). The Imo

Formation is essentially thick clayey shale, fine textured, dark grey to bluish grey with occasional admixture of clay ironstone and thin sandstone beds. The Imo shale range from Paleocene to lower Eocene in age. The Formation is typically dark, very thinly laminated fissile and contains abundant pyrite crystals but poorly fossiliferous (Fayose *et al.,* 1970). The Imo Formation in the eastern part is a lateral equivalent of the Akinbo Formation in Western Nigeria. The Imo Formation outcrops at Okada as Okada shale. Okada clay-shale is therefore part of Imo Formation.

The study area is located in the humid tropical rain forest belt of Nigeria with a mean annual rainfall ranging from 2050 mm to 2161 mm. Temperature values in the area are usually high throughout the year with a minimum annual temperature of 21.90 °C and a mean annual maximum temperature of 25.10 °C. The vegetation of the area is rain forest; however, the original vegetation has been undergoing modifications due to settlement expansion, mining and industrial activities.

### 2.2. Field Sampling

Field data collection was carried out following established standard procedures and practices for environmental data collection in Nigeria by FMENV and recognizing the relevant sections of the Edo State Ministry of Environment guidelines (NSDWQ, 2007). The samples were preserved prior to physical, chemical and biological characteristics analysis.

### 2.3. Water Sampling

Borehole water and surface water samples were collected from the two (2) EU-Borehole projects and Okokpon and Ofunmwengbe streams, which traverse both communities. Surface water was sampled and serve as control. For the boreholes, samples were collected from the waste hot water discharge points (This is the point where water is flowing freely without mechanical pressure from a submersible pumping machine). The borehole projects are situated on a pressurized aquifer and hence there is constant flow of waste hot water even with pressure from a mechanical pump. For the surface water, three sampling stations were established along Okokpon stream and two along Ofunmwengbe stream. The water samples were collected randomly using the grab sampling method by dipping a 250 ml plastic bottle 30 cm below the water surface at each selected sampling point. The sample bottles were labelled in accordance with the appropriate source and date of collection before being transported to the laboratory for analysis. A total of twelve (12) water samples were collected for the study, three from each sampling point (two boreholes and two streams). Each of the twelve samples collected was analyzed for physico-chemical parameters and heavy metals. Sampling was carried out from May to July, 2021.

Plate 1: In-situ measurements using a Hanna portable multi-parameter water parameters

### 2.4. Geophysical Survey Method

The geophysical survey was carried out for two days in the month of July 2021. The work consisted of sensitization of the public on the nature of the work to be carried out. The geophysical survey was carried out using the Earth (Omega-48) resistivity meter (self-averaging-system) and accessories as well as geoscience Analyst software (VES interpretation software). The Earth resistivity meter performs automatic

recording of both voltage and current, stacks the results, computes the resistance in real time and digitally displays it. A hammer was used to pin the electrodes to the ground to about 15 cm to 40 cm depth. Copper rods, which are highly conductive and resistant to corrosion, were used as potential electrodes. To enhance contact and coupling between the current and electrodes, some water was poured on all the electrodes. The array configuration employed was that of Schlumberger which involved injection of current (direct current) into the ground via the current electrodes (two in number) and measuring the corresponding voltage (potential) difference (two in number). From this, the apparent resistivity is delineated from the relation of the measured subsurface Earth resistance and geometric factor (Wightman *et al.,* 2003). The Schlumberger array is very effective in determining the depth characteristics of rock types. This array was selected as the major focus of the survey was to ascertain depth of aquifer and its characteristics. The concept of electrical resistivity is based on the ideal model of a homogeneous (uniform) subsurface condition, based on the mathematical relation in Equations 1 to 4 and Figure 3 show the array arrangement:

$$V = IR \tag{1}$$

$$R = \frac{\rho L}{A} \tag{2}$$

$$\rho a = K.R \tag{3}$$

Thus:

$$\mathrm{K} = \frac{3.142}{2} * (\frac{a^2 - b^2}{b}) \tag{4}$$

a=AB/2 (half-current separation distance) value in meter, b=MN/2 (half-voltage separation distance) value in meter, k= geometric factor, V is voltage, I is current, K is array geometric factor, $\rho a$ is resistivity of the medium, R is resistance, L is Length, and A is the cross-sectional area.

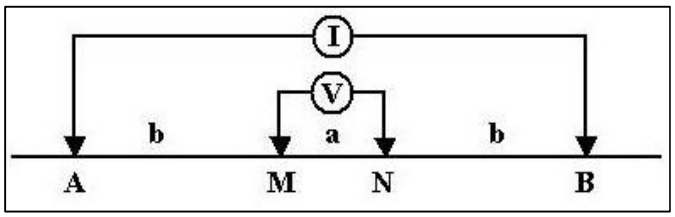


Figure 3: Typical Schlumberger array arrangement

### 2.5. Data Analysis

#### 2.5.1. Laboratory measurement/testing of water quality

Water samples were analysed at Earthquest International Limited, Warri Delta State and Port Harcourt Office, Rivers States. Samples brought to the laboratory were analysed using standard analytical methods. Parameters analyzed include pH, EC, TDS, salinity temperature, TSS, turbidity, chlorine, sulphate, nitrate, nitrite, alkalinity, THC, COD, hardness, phosphate, ammonia, DO, BOD. Cd. Cu, Pb, Fe, Mn, Co, Zn

#### 2.5.2. Geophysical analysis

The set of data gathered was subjected to interpretation using geoscience analyst software. This was followed by a careful geophysical processing involving smoothening (reduction) of the raw from the field. This was achieved using both manual and computer aided approach to eliminate noise, which could lead to spurious anomaly.

#### 2.5.3. Hydropower potentials

Once the potential head drop H (determined from digital elevation model DEM) using GIS and the discharge (Q) of the groundwater determined from pump test are known, the hydro power potential was calculated using Equation 4.

$$P = \rho Q \square h\eta \quad (4)$$

Where P = Power (W), ρ = Density of water (kg/m$^3$), Q = Volumetric fluid flow rate (m$^3$/s), g = gravity constant (9.81 m$^2$/s), h = height (m) of the drop (gross hydro head) and ŋ = efficiency coefficient.

In this study, the density of water was taken as constant at 1,000 kg/m$^3$, the efficiency coefficient was set to 0.8 while the hydro head is defined as the height difference between the intake and the generating station. Thus, with these assumptions, the only two parameters needed are *Q* and *h* to determine the hydropower potentials for the sites in the study.

## 3. RESULTS AND DISCUSSION

### 3.1. Surface Water Quality

The summary of the physicochemical, heavy metals and microbial analyses for the surface water samples is presented in Tables 1 to 3. Most parameters were generally within NSDWQ and WHO limit for the acceptability of water for domestic purpose except for turbidity. The overall result indicates pH was within the desirable and suitable range. pH is determined by the amount of dissolved carbon dioxide ($CO_2$), which forms carbonic acid in water. Present investigation was similar with reports made by other researchers' study (Edimeh *et al*., 2011; Aremu *et al*., 2011).

Table 1: Summary of physico-chemical properties of surface water (Control index)

| Parameter | Range | Mean | NSDWQ | WHO |
|---|---|---|---|---|
| pH | 5.45 - 6.70 | 5.99 | 6.50-8.50 | 6.50-8.50 |
| EC (µS/cm) | 28.75 - 207.50 | 117.06 | 1000.00 | NG |
| TDS (mg/l) | 15.10 - 110.50 | 60.78 | 500.00 | 1000.00 |
| Salinity ($^o/_{oo}$) | 0.01 - 0.06 | 0.03 | | |
| Temperature ($^o$C) | 22.00 - 23.80 | 22.83 | Ambient | Ambient |
| TSS (mg/l) | 23.85 – 54.00 | 38.96 | | 600 |
| Turbidity (NTU) | 28.80 – 71.00 | 46.88 | 5 | 0.2 |
| Chlorine (mg/l) | 5.41 - 30.66 | 17.62 | 250.00 | 250.00 |
| Sulphate (mg/l) | 0.08 - 6.05 | 2.98 | 100 | 250 |
| Colour (Pt.Co) | 39.00 – 83.00 | 60.50 | 15 | 15 |
| Nitrate (mg/l) | 0.06 - 0.15 | 0.11 | 50.00 | 50.00 |
| Nitrite (mg/l) | 0.01 - 0.08 | 0.04 | 0.20 | 3.00 |
| Alkalinity | 12.31 - 32.75 | 22.54 | | |
| THC (mg/l) | BDL | | 150.00 | 500.00 |
| COD (mg/l) | 10.55 - 58.96 | 34.45 | | |
| Hardness | 39.45 - 428.20 | 231.41 | 150 | |
| Phosphate (mg/l) | 0.01 - 0.05 | 0.02 | | |
| Ammonia (mg/l) | 0.25 - 0.41 | 0.32 | | |
| DO (mg/l) | 1.05 - 2.50 | 1.72 | | 3.0 |
| BOD (mg/l) | 0.40 - 2.01 | 1.36 | | 2.0 |

The concentration of TDS in present study was observed in the range of 15.10 and 110.50 mg/l. Water has the ability to dissolve a wide range of inorganic and some organic minerals or salts such as potassium, calcium, sodium, bicarbonates, chlorides, magnesium, sulfates etc. These minerals produce unwanted taste and color in appearance of water. This is the important parameter for the use of water. The water with high TDS value indicates that water is highly mineralized. Desirable limit for TDS is 500 mg/l and maximum limit is 1000 mg/l which prescribed for drinking purpose (WHO, 2011). The mean total dissolved solids

concentration in the study area was found to be 60.8 mg/l, and it is within the limit of WHO standards. Similar value was reported by Meride and Ayenew (2016) in drinking water of Ethiopia. High values of TDS in ground water are generally not harmful to human beings, but may affect persons who are suffering from kidney and heart diseases (NSDWQ, 2007). Water containing high solid may cause laxative or constipation effects (Sasikaran *et al.,* 2012). The fact that turbidity level was high might suggest increased sedimentation and siltation within the river channels. High level of turbidity can indicate the presence of pathogenic microorganisms and be an effective indicator of hazardous events throughout the water supply system, from catchment to point of use (APHA/AWWA/WEF, 2012). Turbidity has no direct health impact but can harbour microorganisms protecting them from disinfection and can entrap heavy metals and biocides (NSDWQ, 2007).

The spatial variation in the physical and chemical parameters of surface water in the study area is presented in Figures 4 and 5 respectively. In Figure 4, it can be seen that electrical conductivity was highest compared to other parameters, even though its levels were within the permissible limit for drinking water. According to Meride and Ayenew (2016), pure water is not a good conductor of electric current rather, it is a good insulator. Increase in ions concentration enhances the electrical conductivity of water. Generally, the amount of dissolved solids in water determines the electrical conductivity. Electrical conductivity actually measures the ionic process of a solution that enables it to transmit current (ISO, 2016). According to WHO standards, the electrical conductivity value should not exceed 400 µS/cm. The current investigation indicated that electrical conductivity value was 117.0.3 µS/cm. A similar finding was reported by Soylak *et al.* (2002) for drinking water of turkey and Meride and Ayenew (2016) which found a mean value of 179.3 µS/cm with an average value of 192.14 µS/cm in Ethiopia respectively. These results clearly indicate that water in the study area was not considerably ionized and has the lower level of ionic concentration activity due to small dissolve solids. In Figure 5, total hardness of water was highest compared to other parameters. Water hardness is the traditional measure of the capacity of water to react with soap, with hard water requiring considerably more soap to produce a lather. Hard water often produces a noticeable deposit of precipitate (e.g. insoluble metals, soaps or salts) in containers, including "bathtub ring" (WHO, 2011). Studies have shown that water hardness is not caused by a single substance but by a variety of dissolved polyvalent metallic ions, predominantly calcium and magnesium cations, although other cations (e.g. aluminium, barium, iron, manganese, strontium and zinc) also contribute (McGowan, 2000). Consequently, the presence of water hardness as seen in the study area could be attributed to the dissolved polyvalent metallic ions from sedimentary rocks. The study area is overlain by sedimentary rock and hence calcium and magnesium, are the two principal ions that are present in many sedimentary rocks. Table 2 buttresses the fact that water hardness as observed in the study area is closely related to the levels of calcium, magnesium and sodium. The role of water hardness has been widely investigated and evaluated for many years in several studies where regional differences in cardiovascular disease have been reported (Masironi *et al.*, 1979; Luoma *et al*., 1983; Rubenowitz *et al.,* 1996; Maheswaran *et al.*, 1999). Previous studies have found positive correlations between water and dietary magnesium and calcium and blood pressure (Dyckner and Wester, 1983; Kesteloot and Joossens, 1988; Sauvant and Pepin 2002; Nerbrand *et al.,* 2003). In Finland and South Africa for example, it was found that the incidence of death ascribed to ischaemic heart disease is inversely correlated with the concentration of magnesium in drinking water (Luoma *et al.,* 1983; Leary *et al.,* 1983). In a study of magnesium in drinking water supplies and mortality from acute myocardial infarction in north-west England, there was likewise evidence of an association between magnesium and cardiovascular mortality (Maheswaran *et al.,* 1999). Figure 6 shows the spatial variation in the concentration of the exchangeable cations in surface water in the project area.

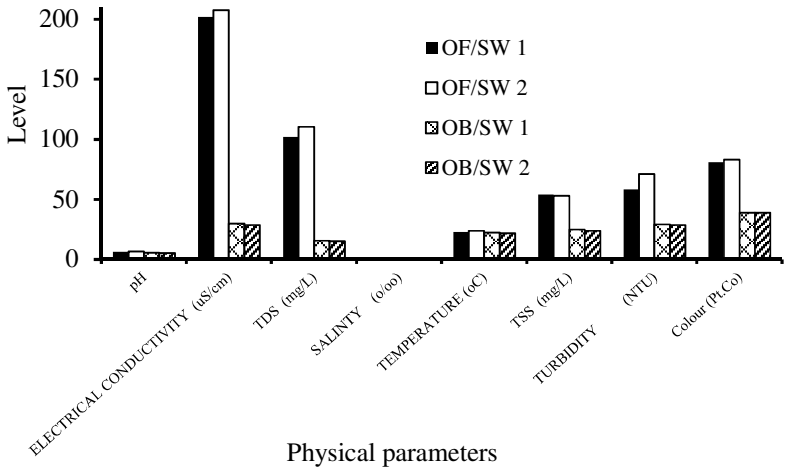


Figure 4: Spatial variation in physical parameters of surface water in the project area (OF/SW: Ofumwengbe surface water; OB/SW: Obaretin surface water)

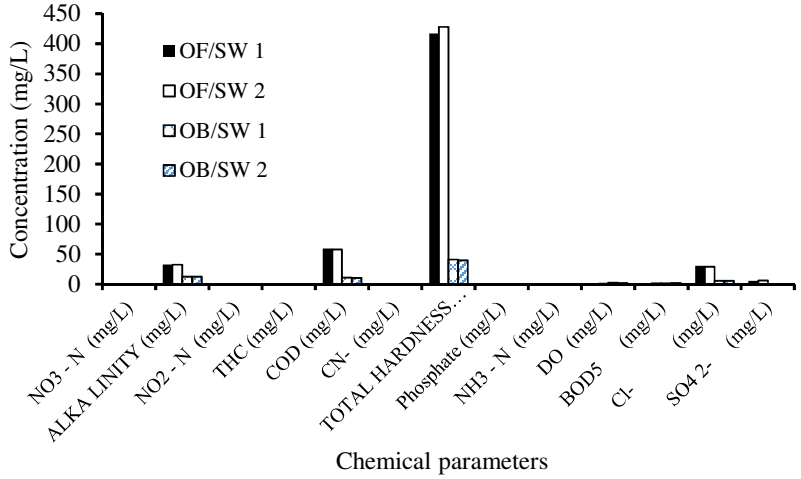


Figure 5: Spatial variation in chemical parameters of surface water in the project area

Table 2: Summary of exchangeable cations concentration in surface water

| Parameter | Range (ppm) | Mean (ppm) |
|---|---|---|
| Ca | 1.44 - 26.03 | 13.48 |
| Mg | 2.50 - 10.06 | 6.22 |
| Na | 5.77 - 71.84 | 38.87 |
| K | 0.08 - 1.21 | 0.60 |

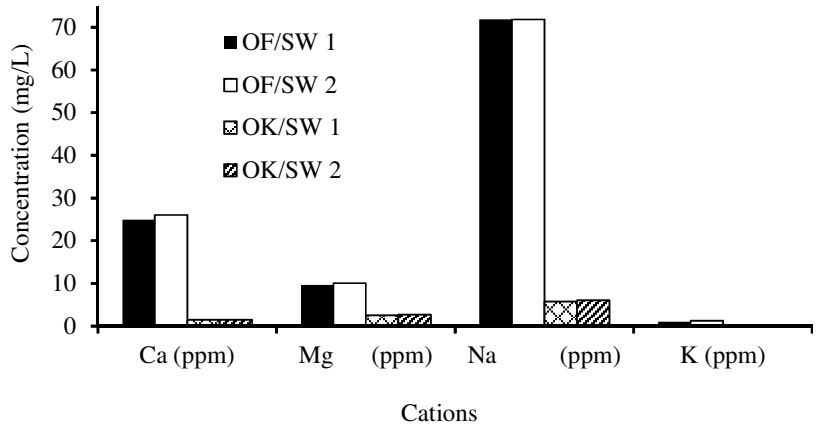


Figure 6: Spatial variation in exchangeable cations concentration

In Table 3, all the heavy metal levels were within standard thresholds of NSDWQ and WHO except for cadmium and iron. Cadmium occurs naturally in zinc, in lead and copper ores, in coal and other fossil fuels, in shales and is released during volcanic action (WHO, 2011). These deposits can serve as sources to ground and surface waters, especially when in contact with low total dissolved solids and acidic waters (WHO, 2011). The study area is underlain by the Imo shale sedimentary rock and thus this may be linked to the level of cadmium in the study area. Cadmium has no biological functions to humans, it has been linked to a number of health problems including renal tubular dysfunction, pulmonary emphysema and possibly Osteomalacia, a situation where calcium in the bones is replaced by Cd in humans which results to cancer of the bones (Jarup and Jarup, 2003). Target organs include liver, placenta, kidneys, lungs, brain and bones (Reilly, 2002). The high concentration of iron above permissible limits may be attributed to geology of the bedrock and other sources of pollution such as such as agricultural and industrial effluents (Butu *et al.,* 2019).

In drinking-water supplies, iron (II) salts are unstable and are precipitated as insoluble iron (III) hydroxide, which settles out as a rust-coloured silt (WHO, 1996). Anaerobic groundwaters may contain iron (II) at concentrations of up to several milligrams per litre without discoloration or turbidity in the water when directly pumped from a well, although turbidity and colour may develop in piped systems at iron levels above 0.05–0.1 mg/litre. Staining of laundry and plumbing may occur at concentrations above 0.3 mg/litre (Department of National Health and Welfare, 1990). Iron is an essential element in human nutrition (WHO, 2011). Estimates of the minimum daily requirement for iron depend on age, sex, physiological status, and iron bioavailability and range from about 10 to 50 mg/day (12). The average lethal dose of iron is 200–250 mg/kg of body weight, but death has occurred following the ingestion of doses as low as 40 mg/kg of body weight (National Research Council, 1979). Autopsies have shown haemorrhagic necrosis and sloughing of areas of mucosa in the stomach with extension into the submucosa (WHO, 1996). Chronic iron overload results primarily from a genetic disorder (haemochromatosis) characterized by increased iron absorption and from diseases that require frequent transfusions (Bothwell, 1979). The spatial concentration of heavy metals in the surface water samples from the project area is presented in Figure 7.

Table 3: Summary of heavy metals concentration in surface water

| Parameter | Range (mg/L) | Mean (mg/L) | NSDWQ (mg/L) | WHO (mg/L) |
|---|---|---|---|---|
| Cd | 0.002 - 0.008 | 0.006 | 0.003 | 0.003 |
| Cu | 0.003 - 0.007 | 0.005 | 1.000 | 2.000 |
| Pb | 0.001 - 0.012 | 0.008 | 0.010 | 0.010 |
| Fe | 0.986 - 1.451 | 1.190 | 0.300 | 0.300 |
| Mn | 0.034 - 0.121 | 0.075 | 20.000 | 0.500 |
| Co | 0.051 - 0.058 | 0.054 | N/A | N/A |
| Zn | 0.014 - 0.018 | 0.016 | 3.0 | 3.000 |

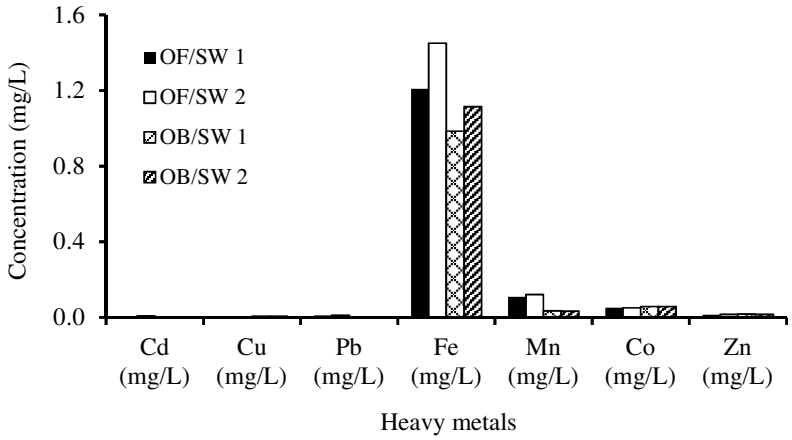


Figure 7: Spatial concentration of heavy metals in surface water samples

### 3.2. EU-Borehole Water Quality

The recorded level of physical and chemical parameters of the borehole water in both communities is presented in Tables 4 and 5, while results of the exchangeable cations and heavy metals quality of the borehole water sample is presented in Tables 6. The temperature of hot water at discharge point ranged between 47.8 ºC and 49.8 ºC. Geothermal resources are classified in various ways based on heat source, type of heat transfer, reservoir temperature, physical state, utilization, and geological settings. When defined on the basis of the nature of the geological system from which they originate, the different categories include volcanic geothermal system, convective fracture-controlled systems, sedimentary geothermal systems, geo-pressured systems, hot dry rock (HDR) or enhanced (engineered) geothermal systems (Saemundsson, *et al.,* 2011; ESMAP, 2012). Adopting the classification, it can be inferred that the hot water from the EU-Borehole did not merit to be classified as volcanic geothermal systems (associated with volcanic activity), convective fracture-controlled systems (tectonically active areas, with above average heat flow) or geo-pressured systems (associated with geo-pressured oil and gas reservoirs). Instead, the observed geothermal reservoirs in the study area are best classified as sedimentary geothermal systems (with respect to the study area, the Imo Formation), a category is found in many of the world's major sedimentary basins. These systems owe their existence to the occurrence of permeable sedimentary layers at great depths (>1 km) and above average geothermal gradients (> 30 ºC/km) (Saemundsson, *et al.,* 2011). These systems are conductive in nature rather than convective, even though fractures and faults play a role in some cases. Some convective systems (such as convective fracture-controlled systems) may, however, be embedded in sedimentary rocks. Similarly, the use of geothermal resources is strongly influenced by the nature of the system that produces them. Hot volcanic systems are utilized primarily for electric power generation, whereas the resources of lower temperature systems are utilized mostly for space heating and other direct uses (ESMAP, 2012). Consideration of a number of factors is required to determine the optimal use of a geothermal resource. These include the type (hot water or steam), rate of flow, temperature, chemical composition, and pressure of the geothermal fluid, and depth of the geothermal reservoir. Geothermal resources vary in temperature from 50 to 350 °C, and can either be dry, mainly steam, a mixture of steam and water or just liquid water. Hydrothermal fields are often classified into high, medium, and low temperature fields. This division is based on inferred temperature at a depth of 1 km; high temperature fields are those where a temperature of 200 °C or more is reached at a depth of 1 km; and low temperature fields are those in which the temperature is below 150 °C at the same depth. High temperature fields are all related to volcanism whereas low temperature fields draw heat from the general heat content of the crust and from the heat flow through the crust. In view of the study findings, it can be concluded that the observed potential geothermal resource in study cannot support electricity generation, but maybe suitable for direct uses such direct heating, hot water

and steam for bathing (recreation), agro-businesses and ground source heating and cooling or small hydropower plant as currently being practiced in most developing counties (Omenda *et al.,* 2019; Dutiro, 2019; Lund and Toth, 2020).

In Table 6, with the exception of Fe and Cr in Obaretin community, all heavy metals analysed in the samples were within acceptable limit for drinking, prescribed by the Nigerian Standard for Drinking Water Quality (NSDWQ, 2007). Chromium is very toxic and mutagenic when inhaled and is a known human carcinogen, and breathing high levels can cause irritation to the lining of the nose, runny nose and breathing problems (Dayan and Paine, 2001).

Table 4: Borehole water physical parameters

| Sample code | pH | EC (uS/cm) | TDS (mg/L) | Salinity ($^{o}/_{oo}$) | Temp. ($^{o}$C) | TSS (mg/L) | Turbidity (NTU) | Colour (Pt.Co) |
|---|---|---|---|---|---|---|---|---|
| OB/BH | 4.50 | 168.00 | 84.40 | 0.07 | 47.80 | 34.0 | 38.6 | 76 |
| OF/BH | 5.50 | 380.00 | 191.40 | 0.06 | 49.80 | 33.0 | 37.3 | 47 |
| NSDWQ limit | 6.5-8.5 | 1000 | 500 | | 25 | | 5.0 | |

Table 5: Borehole water chemical parameters

| Sample code | $Cl^-$ (mg/L) | $SO_4^{2-}$ (mg/L) | $NO_3^-$ (mg/L) | Alkalinity (mg/L) | $NO_2^-$ (mg/L) | THC (mg/L) | COD (mg/L) | $CN^-$ (mg/L) | Total hardness (mg/L) | Phosphate (mg/L) | $NH_3^-$ (mg/L) | DO (mg/L) | $BOD_5$ (mg/L) |
|---|---|---|---|---|---|---|---|---|---|---|---|---|---|
| OB/BH | 35.43 | 11.253 | 0.336 | 3.00 | 0.037 | <0.1 | 14.93 | <0.1 | 215.0 | 0.025 | 0.135 | 1.90 | 0.40 |
| OF/BH | 31.64 | 13.260 | 0.037 | 12.20 | 0.015 | <0.1 | 121.36 | 0.63 | 567.0 | <0.001 | 0.247 | 0.00 | 2.20 |

Table 6: Borehole water cations and heavy metal concentrations

| Sample code | $Cr^{-6}$ (mg/L) | Cd (mg/L) | Cu (mg/L) | Pb (mg/L) | Fe (mg/L) | Ni (mg/L) | Mn (mg/L) | Co (mg/L) | V (mg/) | Zn (mg/L) | As (mg/L) | Ca (ppm) | Mg (ppm) | Na (ppm) | K (ppm) |
|---|---|---|---|---|---|---|---|---|---|---|---|---|---|---|---|
| OB/BH | 0.072 | 0.003 | 0.010 | <0.001 | 3.208 | <0.005 | 0.089 | 0.024 | <0.05 | 0.016 | <0.05 | 24.520 | 9.705 | 75.500 | 1.033 |
| OF/BH | <0.001 | 0.007 | <0.001 | <0.001 | 4.554 | <0.005 | 0.055 | 0.050 | <0.05 | 0.009 | <0.05 | 49.440 | 10.206 | 168.100 | 1.756 |
| NSDWQ | 0.05 | 0.003 | 1.0 | 0.01 | 0.3 | 50 | 0.2 | - | - | - | - | | | | |

### 3.3. Geophysical Data Presentation and Interpretation

The surface geophysical electrical data with respect to the response curve generated indicated range of hybrid curves (QHK to HK) for both communities as seen in Figures 8 and 9. Analysis from geophysical perspective indicated a maximum of five (5) geo-electric layers and revealed top soil of varying thickness, lateritic layer, as well as clay/silty/ clayey sandy layer unit of low porosity and permeability, and finally sandy layer (porous and permeable), which is the targeted saturated zone of interest. These layers were fragmented into sub-layers to assure confidence on the modeled surface geophysical data. The various resistivity curves processed, reflect QHK to HK curves for both. Geologic materials inferred are sandy, silty sand, clayey sandy, sandy clayey and pure clayey (claystone) materials, with high degree of ferrugenisation, dominating at the shallow stratigraphic zone of the study area as seen in Tables 7 and 8. At Ofunmwengbe, top of the aquifer was seen to prime at 317 m depth, due to principle of equivalence and suppression, the base part was masked (not fully imaged), while at Obarentin the nasal part of the aquifer was resolved and seen to prime at 342 m depth.

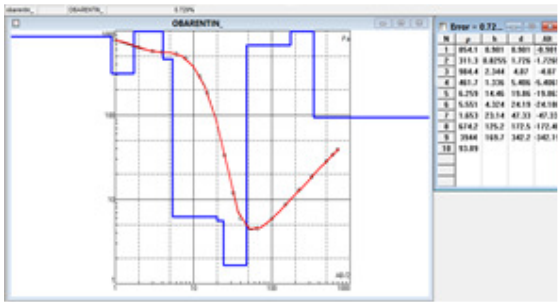

Figure 8: A graphical representation of VES 1 Data layer model

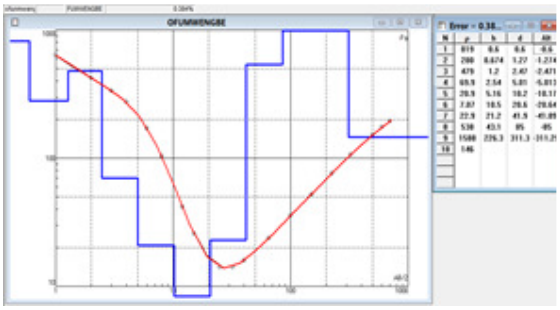

Figure 9: A graphical representation of VES 2 Data layer model

Table 7: Layer model of VES 1 (Obaretin) parameters with geologic inference

| | RESISTIVITY (Ωm) | THICKNESS (m) | DEPTH (m) | ELEVATION (Ref: 0 m) | GEOLOGIC INFERENCE | |
|---|---|---|---|---|---|---|
| OBARENTIN EARTH MODEL | 854.10 | 0.901 | 0.901 | -0.901 | Top soil | Thick Lateritic (ferruginised zone) |
| | 311.30 | 0.826 | 1.727 | -1.727 | Sandy Clayey layer | |
| | 984.40 | 2.344 | 4.071 | -4.071 | Perched Shallow aquifer | |
| | 461.70 | 1.336 | 5.407 | -5.407 | | |
| | 6.26 | 14.460 | 19.867 | -19.867 | Clay layer | |
| | 5.55 | 4.324 | 24.191 | -24.191 | | |
| | 1.65 | 23.140 | 47.331 | -47.331 | | |
| | 674.20 | 125.200 | 172.531 | -172.531 | Clayey/silty clay/sandy clay layer (Heterolith) | Vadose zone |
| | 3944.00 | 169.700 | 342.231 | -342.231 | **Targeted zone (Aquifer)** | Phreatic zone |
| | 93.89 | ∞ | ∞ | ∞ | Aquitard | Aquitard |

Table 8: Layer model of VES 2 (Ofumwengbe) parameters with geologic inference

| | RESISTIVITY (Ωm) | THICKNESS (m) | DEPTH (m) | ELEVATION (Ref: 0 m) | GEOLOGIC INFERENCE | |
|---|---|---|---|---|---|---|
| OFUMWENGBE EARTH MODEL | 819.00 | 6.000 | 6.000 | -6.000 | Top soil | Thick Lateritic (ferruginised zone) |
| | 280.00 | 0.674 | 6.674 | -6.674 | Sandy Clayey layer | |
| | 479.00 | 1.200 | 7.874 | -7.874 | Perched Shallow aquifer | |
| | 69.90 | 2.540 | 10.414 | -10.414 | | |
| | 20.90 | 5.160 | 15.574 | -15.574 | Clay layer | |
| | 7.07 | 10.500 | 26.074 | -26.074 | | |
| | 22.90 | 21.200 | 47.274 | -47.274 | | |
| | 538.00 | 43.100 | 90.374 | -90.374 | Clayey/silty clay/sandy clay layer (Heterolith) | Vadose zone |
| | 1588.00 | 226.300 | 316.674 | -316.674 | **Targeted zone (Aquifer)** | Phreatic zone |
| | 146.00 | ∞ | ∞ | ∞ | Aquitard | Aquitard |

### 3.4. Assessment of Head at Discharge Points

Head is the vertical distance between two points (intake and turbine). It can also be defined as the pressure created by elevation difference between intake and turbine. In the two locations (Obaretin and Ofumwengbe) the potential head drops were computed. In this study, the approach was to overlay the digital elevation model (DEM) map of the basin and the river network shape file and obtain the raster value within the area.

The difference between the raster values within the sub basin gives the potential head drop in the project locations. Figures 10 and 11 show the digital elevation models of the two locations while Figures 12 and 13 show the 5 m contour interval of the sites. To provide a suitable allocation for hydroelectric power stations installation, it is important to evaluate the characteristics of water resources such as the head and the discharge in different areas of the river. Therefore, these two issues must also be considered (Tian *et al.,* 2020). Thus, one most important factor for the hydraulic heads is the topography of watershed and the position of the intake and the turbine. The hydraulic head is the height difference between the two points in the up and down of the river, also the vertical height difference between the intake and the turbine is called the head (Emeribe *et al.*, 2016). Based on the digital elevation model map, wherever the height difference between the two points is high (the slope of the area is high), the amount of head hydraulic is high, therefore according to Bernoulli's formula, potential energy is converted into kinetic energy and this converted into kinetic energy Moving downstream of the turbine increases power output (Zhou *et al.*, 2020). The contour intervals of the study are indication of fairly distributed heights and provide information concerning the slope characteristics of the study area and thus the first steps used to compute the height difference the intake and the turbine for all proposed places.

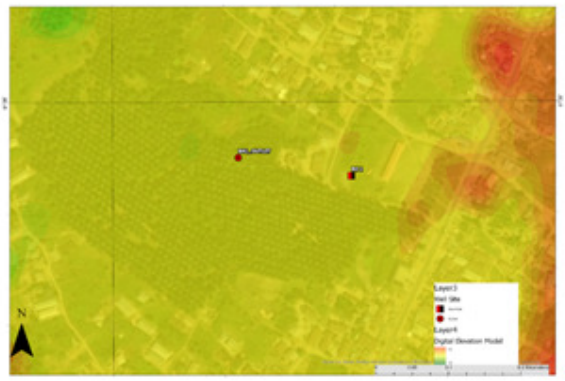

Figure 10: DEM of Obaretin

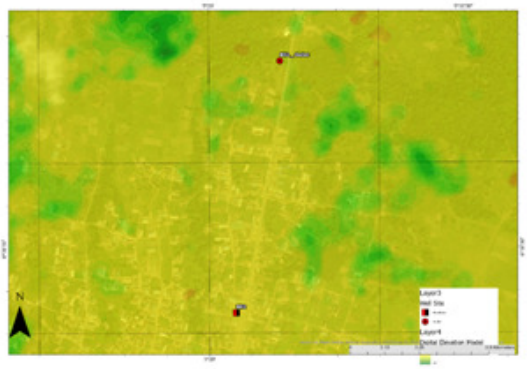

Figure 11: DEM for Ofumwengbe

Figure 12: 5 m Contour interval of Obaretin

Figure 13: 5 m Contour Interval of Ofumwengbe

### 3.5. Slope/Elevation Determination at Discharge Points

The elevation raster was generated from the DEM using the create elevation tools. Slope classes were also generated using the slope tools out of spatial analyst tool box. A DEM with a resolution of 90 m at the equator is available free of charge at the homepage of the Consortium of Spatial information (CGIAR). This data was acquired during the Shuttle Radar Topography Mission (SRTM). The needed tiles of the SRTM

90m DEM version 4product was downloaded in image format. The data was then projected in a geographic (lat/long) projection, with the WGS84 horizontal datum and the EGM96 vertical datum. For the slope computations to be in linear units of meters, the DEM was projected with the project raster tool (Data management toolbox) in ArcGIS into UTM 32N. Then slope classes were generated using the slope tool out of the Spatial Analyst Toolbox. Figures 14 and 15 show the elevation at the project sites.

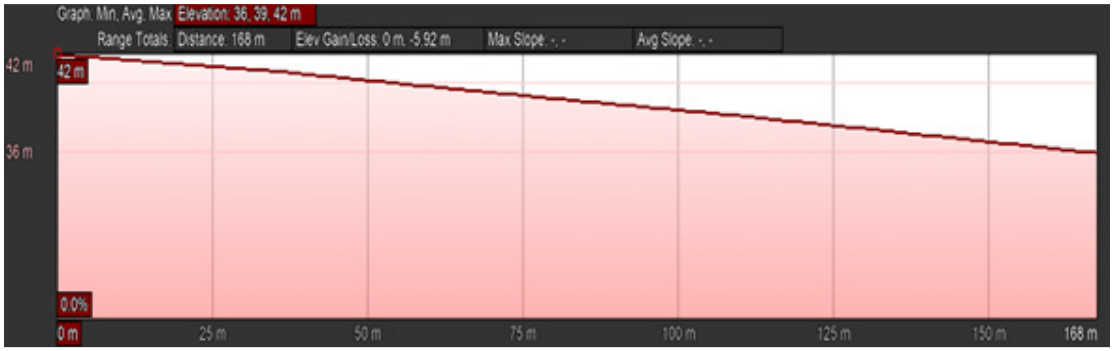


Figure 14: Elevation profile generated from digital elevation model for Obaretin

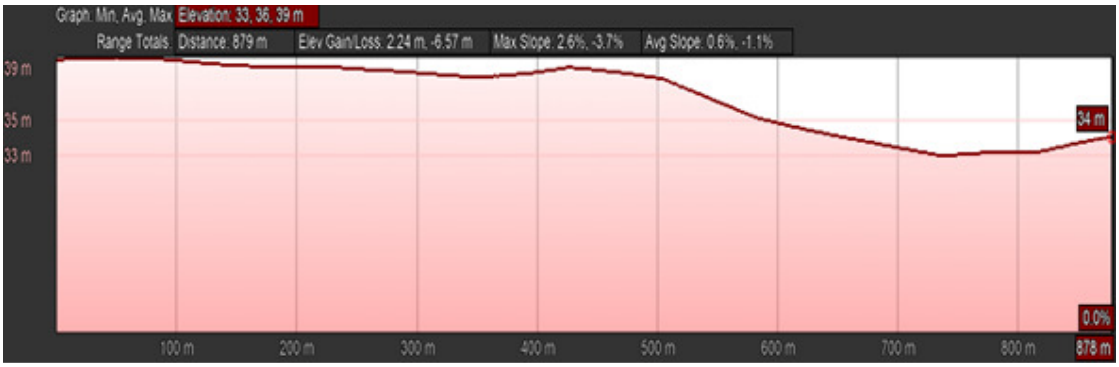


Figure 15: Elevation profile generated from digital elevation model for Ofumwengbe

The elevation profile of the study area also give some insight into the slope characteristic of the study area. The portions with strong slopes will lead to faster discharge which travel only a short distance. Hydropower is produced from a generator driven by water turbines that convert the energy of fast-flowing water into mechanical energy. Water at a higher elevation flows downward through large pipes or tunnels (penstocks). The falling water rotates turbines, which drive the generators. The generator in turn converts the turbines mechanical energy into electricity. The quantity of water as well as the available head determines the production of the hydropower (Paish, 2002).

### 3.6. Power Potential Hot Water at Discharge Points

From pumping test carried out at the borehole locations, the results revealed that Obaretin has an average discharge of 8.9 $m^3/h$ (0.00247 $m^3/s$) while the average discharge at Ofumwengbe was estimated to be 8.6 $m^3/h$ (0.00234 $m^3/s$). Using the above information and applying Equation (4), the power potentials of the two locations within the study area was estimated to be 116.31 W and 147 W from Obaretin and Ofumwengbe respectively (Table 9).

Table 9: Summary of topography, discharge volume and power potential from EU-Borehole at discharge points

| Site | Elevation at well head (m) | Elevation at well outlet (m) | Average slope well head to outlet (%) | Average discharge | Power potentials |
|---|---|---|---|---|---|
| Obaretin (BH1) | 42 | 36 | 4.8 | 8.9 $m^3/h$ (0.00247 $m^3/s$) | 116.31 W |
| Ofumwengbe (BH2) | 40 | 32 | 0.6 | 8.6 $m^3/h$ (0.00234 $m^3/s$) | 147.00 W |

## 4. CONCLUSION

The present study aimed to investigate the potentials for the development of geothermal energy resources from EU-borehole water scheme projects in Obaretin and Ofumwengbe Communities, Ovia South West, Edo State. The study concludes that the observed potential geothermal resource in study area cannot support electricity generation which requires a temperature as high as 200 °C (power generation with conventional steam, flash, double flash, or dry steam technology in areas on the boundaries of tectonic plates, on hot spots and volcanic areas), but instead may be suitable for direct uses such direct heating, hot water and steam for bathing, agro-businesses and ground source heating and cooling or small hydropower plant all of which will boost the economy of the community whose livelihood is mainly peasant farming. The hot water from the EU-Borehole did not merit to be classified as 1) volcanic geothermal systems (associated with volcanic activity) 2) convective fracture-controlled systems (tectonically active areas, with above average heat flow) or 3) geo-pressured systems (associated with geo-pressured oil and gas reservoirs). Instead, the observed geothermal reservoirs in the study area is best classified as sedimentary geothermal systems (With respect to the study area, the Imo Formation) which are found in many of the world's major sedimentary basins.

## 5. ACKNOWLEDGEMENT

This study was funded by the Energy Commission of Nigeria. The authors are thus grateful to the Director-General, Prof. E.J Bala and the Technical Advisory Committee of the National Centre for Energy and Environment, University of Benin for approving funds to embark on this study.

## 6. CONFLICT OF INTEREST

There is no conflict of interest associated with this work.

## REFERENCES

Andrianaivo, L and Ramasiarinoro V.J. (2015). Geothermal Energy Resources of Madagascar - Country Update. *Proceedings of the World Geothermal Congress Melbourne, Australia*, 19-25 April 2015

Aremu, M.O., Olaofe, O., Ikokoh, P.P., and Yakubu, M.M. (2011). Physicochemical characteristics of strem, well and borehole water sources in Eggon, Nasarawa State, Nigeria. *Journal Chemical Society Nigeria*, 36 (1), 131-136.

APHA/AWWA/WEF. (2012). *Standard method 2130: Turbidity*. Standard methods for the examination of water and wastewater, 22nd edition. Washington, DC: American Public Health Association, American Water Works Association and Water Environment Federation.

Bothwell, T.H., Charlton, R.W., Cook, J.D. and Finch. C.A. (1979). *Iron Metabolism in Man.* Blackwell Scientific Publications, Oxford. p. 576.

Butu, A.W., Bello, M.I., Atere, P.M. and Emeribe, C.N. (2019). Assessment of Heavy Metals Pollution in the Surface Water from Thomas Dam, Kano State, Nigeria. *Nigerian Research Journal of Engineering and Environmental Sciences,* 4(2), pp. 789-800

Dayan, A.D. and Paine, A.J. (2001). Mechanisms of chromium toxicity, carcinogenicity and allergenicity: Review of the literature from 1985 to 2000. *Human and Experimental Toxicology*, 20, pp. 439-451

Department of National Health and Welfare (1990). Nutrition recommendations. *The report of the Scientific Review Committee*. Ottawa, Canada.

DiPippo, R (1991). Geothermal energy Electricity generation and environmental impact. *Energy Policy,* 19 (8), pp. 798-807

Dutiro, L. (2019). *The Power of the unknown: Geothermal energy in Zimbabwe*. The Chronicle

Dyckner, T. and Wester, P.O. (1998). Effect of magnesium on blood pressure. *British Medical Journal (Clinical Research Education)*, 286(184), pp. 7-9

Edimeh, P.O., Eneji, I.S., Oketunde, O.F. and Sha'ato, R. (2011). Physico-chemical parameters and some Heavy metals content of Rivers Inachalo and Niger in Idah, Kogi State. *Journal Chemical Society Nigeria,* 36(1), pp. 95-101.

Emeribe, C.N., Ogbomida E.T., Fasipe, O.A., Biose, O., Isiekwe, M., Aganmwonyi, I., and Fasipe I. P. (2016). Hydrological Assessments of Rivers for Small-Scale Hydropower Development in Edo State, Nigeria. *Nigerian Journal Technology,* 35 (3), pp. 656-668

Emofurieta, W.O., Ogundimu, F.O. and Imeokparia, E.G., (1994). Mineralogical Geochemical and Economic Appraisal of some clay and shale deposits in South western and North Eastern Nigeria. *Journal of Mining Geology*, 30(2), pp. 151-159.

Energy Information Administration (EIA) (2021). *Annual Energy Outlook 2021. U.S.* Energy Information Administration of the outlook for energy markets through 2050

Energy Commission of Nigeria (ECN) (2003). *National Energy Policy*. Federal Republic of Nigeria, Abuja.

Energy Sector Management Assistance Program (ESMAP), (2012). Geothermal Handbook: Planning and Financing Power Generation. *Technical Report* 0 0 2 / 12. 1818 H Street, NW Washington DC 20433 USA

ESI Africa (2019). Geothermal energy: The champion of East Africa's thermal prosperity. *ESI Africa Issue* 3-2019.

Fayose, E.A. (1970). Stratigraphic Paleontology of Afowo 1 well, S.W Nigeria. *Journal of Mining Geology,* 5(1), pp. 1-99

International Energy Agency (IEA) (2013). *World Energy Outlook 2013*. IEA, Paris.

International Renewable Energy Agency (IRENA) (2020). *Renewable capacity statistics 2020.* International Renewable Energy Agency (IRENA), Abu Dhabi

International Standard Organization (ISO) (2016). *International Standard ISO 7027–1:2016(E): Water quality – determination of turbidity*. Part 1: quantitative methods. Geneva: International Organization for Standardization.

Jarup, L. and Järup, L. (2003). Hazards of heavy metal contamination. *British Medical Bulletin*, 68(1), pp. 167–182.

Kesteloot, H. and Joossens, J.V. (1988) Relationship of dietary sodium, potassium, calcium, and magnesium with blood pressure. *Belgian Interuniversity Research on Nutrition and Health. Hypertension*, 12 (5), pp 94-9

Kwaya, M.Y. and Kurowska, E. (2020). *Geothermal Energy Resource Potential of Nigeria's Sedimentary Basins.* Proceedings of the World Geothermal Congress 2020. Reykjavik, Iceland, 12 p.

Leary, W.P., Reyes, A.J., Lockett, C.J., Arbuckle, D.D. and van der Byl, K. (1983). Magnesium and deaths ascribed to ischaemic heart disease in South Africa. A preliminary report. *South African Medical Journal,* 64(77), pp. 5- 6

Lund, J.W. and Toth, A.N. (2020). *Direct Utilization of Geothermal Energy 2020 Worldwide Review.* Proceedings of the World Geothermal Congress 2020 Reykjavik, Iceland, April 26 – May 2, 2020

Luoma, H., Aromaa, A., Helminen, S., Murtomaa, H., Kiviluoto, L., Punsar, S. and Knekt, P. (1983). Risk of myocardial infarction in Finnish men in relation to fluoride, magnesium and calcium concentration in drinking water. *Acta Medica Scandinavica.* 213 pp171-6

McGowan, W. (2000). *Water processing: residential, commercial, light-industrial*, 3rd ed. Lisle, IL, Water Quality Association.

Maheswaran, R., Morris, S., Falconer, S., Grossinho, A., Perry, I., Wakefield, J. and Elliott, P. (1999). Magnesium in drinking water supplies and mortality from acute myocardial infarction in north west England. *Heart*, 82(4), pp. 55-60

Masironi R., Pisa, Z., and Clayton D (1979). Myocardial infarction and water hardness in the WHO myocardial infarction registry network *Bulletin of World Health Organization*, 57, pp. 291-9.

Meride, Y., and Ayenew, B. (2016). Drinking water quality assessment and its effects on residents health in Wondo genet campus, Ethiopia. *Environmental Systems Research*, 5 (1), pp. 1-7.

Nerbrand, C., Agréus L., Lenner R.A., Nyberg, P. and Svärdsudd, K. (2003). The influence of calcium and magnesium in drinking water and diet on cardiovascular risk factors in individuals living in hard and soft water areas with differences in cardiovascular mortality. *BMC Public Health*, 3(1), pp. 1-9.

Nigerian Standard for Drinking Water Quality (NSDWQ), (2007). *Nigerian Standard for Drinking Water.* Nigerian Industrial Standard, NIS: 554, pp. 13-14

National Research Council (1979). *Iron*. Baltimore, MD, University Park Press

Oduor, J.A. (2010). Environmental and Social Considerations in Geothermal Development. *Facing the Challenges – Building the Capacity Sydney*, Australia, 11-16 April 2010

Omenda, P., Mangi, P., Ofwona, C. and Mwangi, M. (2020). *Country Update Report for Kenya 2015-2019,* Proceeding, World Geothermal Congress 2020, Reykjavik, Iceland, 16 p.

Reilly, C. (2002*). Metal contamination of food.* Blackwell Science Limited. USA, 81-194.

Paish, O. (2002). Small hydro power: technology and current status. *Renewable and Sustainable Energy Review,* 6(6), pp. 537–556

Rubenowitz, E., Axelsson, G. and Rylander, R. (1996). Magnesium in drinking water and death from acute myocardial infarction *American Journal of Epidemiology*, 143(4), pp. 56-62

Saemundsson, K., Gudni, A. and Benedikt, S. (2011). *Geothermal Systems in Global Perspective*. ÍSOR—Iceland GeoSurvey, January.

Sasikaran, S., Sritharan, K., Balakumar, S. and Arasaratnam, V. (2012). Physical, chemical and microbial analysis of bottled drinking water. *Ceylon Medical Journal*, 57(3), pp. 111–116.

Sauvant., M.P. and Pepin, D. (2002). Drinking water and cardiovascular disease Food. *Chemical Toxicology,* 40(13), pp. 11-25.

Soylak, M., Divrikli, U., Saracoglu, S. and Elci, L. (2002). Monitoring trace metal levels in Yozgat-Turkey: Copper, iron, nickel, cobalt, lead, cadmium, manganese and chromium levels in stream sediments. *Polish Journal of Environmental Studies*, 11, pp. 47-51.

Tian, Y., Zhang, F., Yuan Z., Che, Z. and Zafetti, N. (2020). Assessment power generation potential of small hydropower plants using GIS software *Energy Reports,* 6, pp. 1393–1404

Wightman, W. E., Jalinoos, F., Sirles, P. and Hanna, K. (2003). *Application of Geophysical Methods to Highway Related Problems.* Federal Highway Administration, Central Federal Lands Highway Division, Lakewood, CO, Publication No. FHWA-IF-04-021. http://www.cflhd.gov/resources/agm/Exit EPA Disclaimer

World Health Organization (WHO) (1996). *Iron in Drinking-water*: Guidelines for drinking-water quality, 2nd ed. Vol. 2. Health criteria and other supporting information. World Health Organization, Geneva.

World Health Organization (WHO) (2011). *Guidelines for drinking-water quality*, 4th Ed. Geneva, Switzerland

United Nations Environment Programme (UNEP) (2020). Iceland, a world leader in clean energy, supports Africa's push for geothermal power.

Zhou Y., Guo, S., Xu, C., Chang, F., Chen, H., Liu P. and Ming B. (2020). Stimulate hydropower output of mega cascade reservoirs using an improved Kidney Algorithm. *Journal of Cleaner Production*, 244, p. 118613.